small
NANO MICRO

Compact Halo-Ligand-Conjugated Quantum Dots for Multicolored Single-Molecule Imaging of Overcrowding GPCR Proteins on Cell Membranes

Akihito Komatsuzaki, Tatsuya Ohyanagi, Yoshikazu Tsukasaki, Yukihiro Miyanaga, Masahiro Ueda, and Takashi Jin**

Single-molecule fluorescence imaging has become a standard technique for acquiring exquisite details of diffusion-mediated cellular processes in living cells.[1,2] This imaging requires very bright and robust probes, because photobleaching by excitation light often obscures the individual trajectories of the targeted molecules. Traditional fluorescent probes based on organic dyes and fluorescent proteins are particularly susceptible to photobleaching, whereas semiconductor quantum dot (QD)-based fluorescent probes are far less so.[3] In addition, QDs with different emission wavelengths allow for relatively easy multicolored fluorescence imaging by a single excitation-light source, making them ideal when investigating molecular dynamics in living cells.[4,5] In this paper, we report HaloTag-ligand[6] conjugated QDs (Halo-QDs) with a compact size (<6 nm) for multicolored single-molecule imaging of GPCR membrane proteins on living cells. The HaloTag ligand is a halo-alkane compound that forms a covalent bond with a HaloTag protein (HTP) viaa nucleophilic attack on Asp106 of HTP.[7]

In the single-molecule imaging, the optical resolution is restricted by the diffraction limit of the fluorescence emission wavelength, which is approximately 200 nm when using visible light. Thus, under the condition of high density of fluorescent molecules, it is difficult to discriminate individual single-molecules existing within the diffraction limit by using single-colored fluorescence imaging. To overcome this problem, we developed multicolored single-molecule imaging using compact Halo-QDs to observe overcrowding membrane proteins that exist within the optical diffraction limit. For the single-molecule imaging of membrane proteins, Liu et al. recently reported a two-step conjugation method for labeling membrane proteins with QDs.[8] They introduced HaloTag ligands to membrane proteins using lipoic acid ligase, and then reacted these ligands with HTP-labeled QDs. In this case, the size of HTP conjugated QDs should be larger than the original QDs before conjugation, where the molecular weight of HTP is 33 kDa.[7] For the labeling of membrane proteins, smaller probes are suitable for decreasing their effect on the diffusion and enzymatic activity of the proteins. Rao et al. first reported HaloTag ligand conjugated QDs[9] for the labeling of HTP-luciferase fusion proteins, where commercially available amino-HaloTag ligands were used to conjugate the ligands to the surface of the QDs by carbodiimide chemistry. However, labeling efficiency using this method is not ideal. The labeling of HaloTag ligands on QDs with high efficiency often results in colloidal instability of the QDs in aqueous solution owing to the hydrophobicity of the HaloTag ligands, complicating biological studies. At the same time, when the labeling efficiency is very low, the binding activities of HaloTag ligand-conjugated QDs to HTP decrease. The group later reported another labeling method for preparing HTP-fused proteins using streptavidin-conjugated QDs.[10] They first labeled HTP with biotinylated HaloTag ligands, which were then reacted with streptavidin-conjugated QDs. Using this method, they successfully performed cellular imaging of platelet-derived growth factor receptors in COS7 cells. However, they did not demonstrate if their QD labeling method is viable for single-molecule imaging. In this work, we developed a facile synthetic method for preparing Halo-QDs with a compact size (<6 nm) for the multicolored single-molecule imaging of GPCR proteins.

To prepare compact Halo-QDs for single molecule imaging, we synthesized a thiol-terminated HaloTag-ligand (Halo-SH) that directly bind to the surface of the QDs (**Scheme 1**a, and SI, Figure S1). This HaloTag-ligand enables quantitative control of the molecule number of HaloTag ligands presented on the QD surface. To introduce quantitative amounts of the Halo-SH ligand on the QD surface, we used ligand exchange in trioctylphosphine oxide (TOPO)-coated

A. Komatsuzaki, Dr. T. Ohyanagi, Dr. Y. Tsukasaki, Dr. T. Jin
Laboratory for Nano-Bio Probes
Quantitative Biology Center, Riken
Suita 565–0874, Osaka, Japan
E-mail: tjin@riken.jp
Dr. Y. Miyanaga, Prof. M. Ueda
Laboratory for Cell Signaling Dynamics
Quantitative Biology Center, Riken
Suita 565–0874, Osaka, Japan
E-mail: ueda@bio.sci.osaka-u.ac.jp
Dr. Y. Miyanaga, Prof. M. Ueda
Laboratory of Single Molecule Biology
Department of Biological Sciences
Graduate School of Science,
Osaka University
Toyonaka 560–0043, Osaka, Japan

DOI: 10.1002/smll.201402508

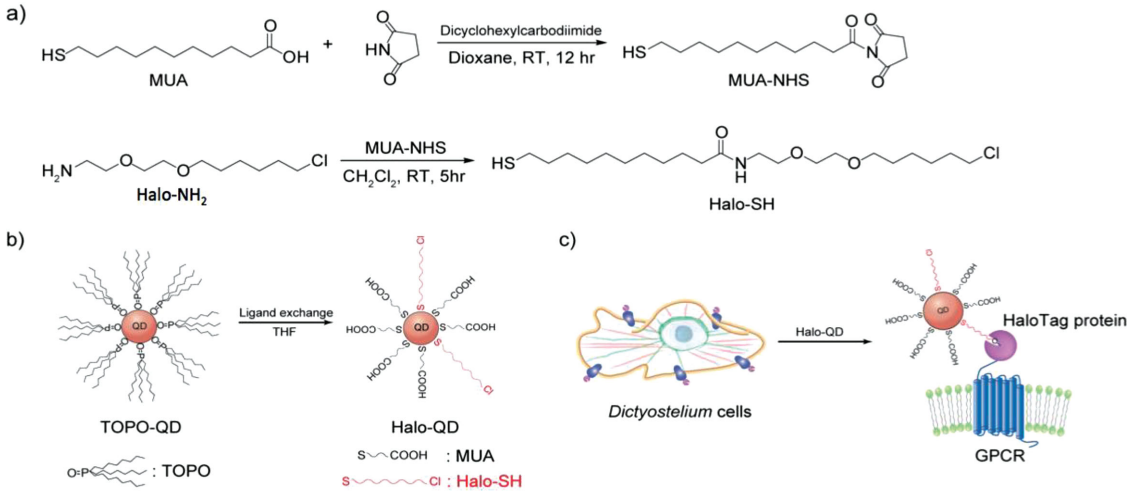

Scheme 1. (a) Synthesis of HaloTag ligand (Halo-SH). (b) Schematic of the ligand exchange of TOPO-coated QDs with a mixture of MUA and Halo-SH in tetrahydrofuran at RT. (c) Schematic of the specific labeling of GPCR proteins by Halo-QDs.

QDs using a mixture of mercaptoundecanoic acid (MUA) and Halo-SH (Scheme 1b). In this ligand exchange reaction, we can vary the amounts of Halo-SH molecules on the QD surface by changing the ratio of Halo-SH to MUA. Using the QDs capped with Halo-SH and MUA molecules, we successfully labeled HTP-fused cAR1 receptors in *Dictyostelium* cells[11,12] (Scheme 1c). The cAR1 receptor is a GPCR protein at membrane surface to recognize cyclic adenosine monophosphate in chemotaxis of the *Dictyostelium* cells.[13]

Highly fluorescent QDs (CdSe/ZnS and CdSeTe/CdS) were synthesized using high-temperature decomposition[14] of organometallic compounds in TOPO as a protecting agent, followed by coating the surface of the QDs with a mixture of MUA and Halo-SH. Since Halo-SH is a hydrophobic molecule and not soluble in water, high contents of Halo-SH presented on the QD surface often result in aggregation of the QDs in aqueous solution. Thus, optimization of the content ratio of Halo-SH used for the surface coating is needed to obtain water-soluble Halo-QDs with high dispersibility. To check the colloidal stability of QDs in water, we used fluorescence correlation spectroscopy (FCS), which provides the diffusion coefficients of the QDs in aqueous solution.[15] Using the Stokes-Einstein relationship, the diffusion coefficients can be used to evaluate the hydrodynamic diameters of the Halo-QDs. The hydrodynamic diameter of Halo-QDs strongly depended on the content ratio of Halo-SH used for the ligand exchange (**Figure 1**). The diameter of Halo-QDs was insensitive to a mol percent of Halo-SH <10%, but very sensitive at >25%. At 100 mol% of Halo-SH in the ligand-exchange reaction (Scheme 1b), we could not measure the hydrodynamic diameter of the Halo-QDs due to aggregation of the QDs in aqueous solution. To check the monodispersibility of the Halo-QDs, we measured the dependence of fluorescence intensity (count per molecule, CPM) of Halo-QDs, showing that the CPM value of Halo-QDs is almost constant at a mol percent of Halo-SH <10% (Inset Figure 1). This finding shows that the Halo-QDs (QD525) are monodispersed particles with a hydrodynamic diameter of ca. 4 nm in aqueous solution at a mol percent of Halo-SH <10%.

To achieve multicolored single-molecule fluorescence imaging, we prepared three types of QDs on which the HaloTag ligands are presented (Halo-SH: MUA = 10:90 molar ratio): emission at 525 nm (QD525, CdSe/ZnS), at 600 nm (QD600, CdSe/ZnS), and at 700 nm (QD700, CdSeTe/CdS). Fluorescence spectra of the three types of QDs in phosphate buffer are shown in **Figure 2**a. These QDs were well dispersed in aqueous solution (pH = 8), and QD aggregation was not observed over one week (SI, Figure S2). Fluorescence correlation curves for the three QDs were fitted with a single-component diffusion model,[15] and their hydrodynamic diameters were determined to be 4.2 nm, 5.5 nm, and 6 nm for QD525, QD600, and QD700, respectively (Figure 2b). To confirm the binding ability of the Halo-QDs (QD600) to HaloTag fusion proteins, we measured the size of the Halo-QDs after the binding of the fusion

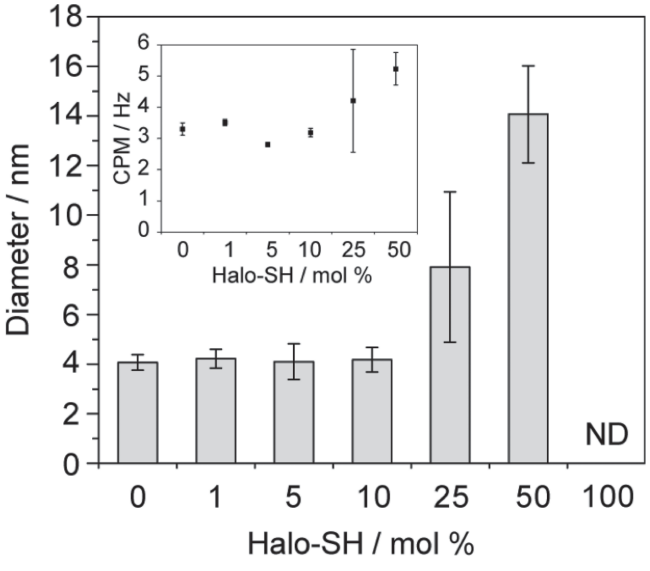

Figure 1. Dependence of the hydrodynamic diameter of Halo-QDs (QD525) on the mol percent of Halo-SH ligand ([Halo-SH]/[Halo-SH+MUA]) used for the ligand exchange of TOPO-coated QDs. ND: not determined. Inset shows the dependence of fluorescence intensity (count per molecule, CPM) of Halo-QDs on the mol% of Halo-SH.

small 2014,
DOI: 10.1002/smll.201402508

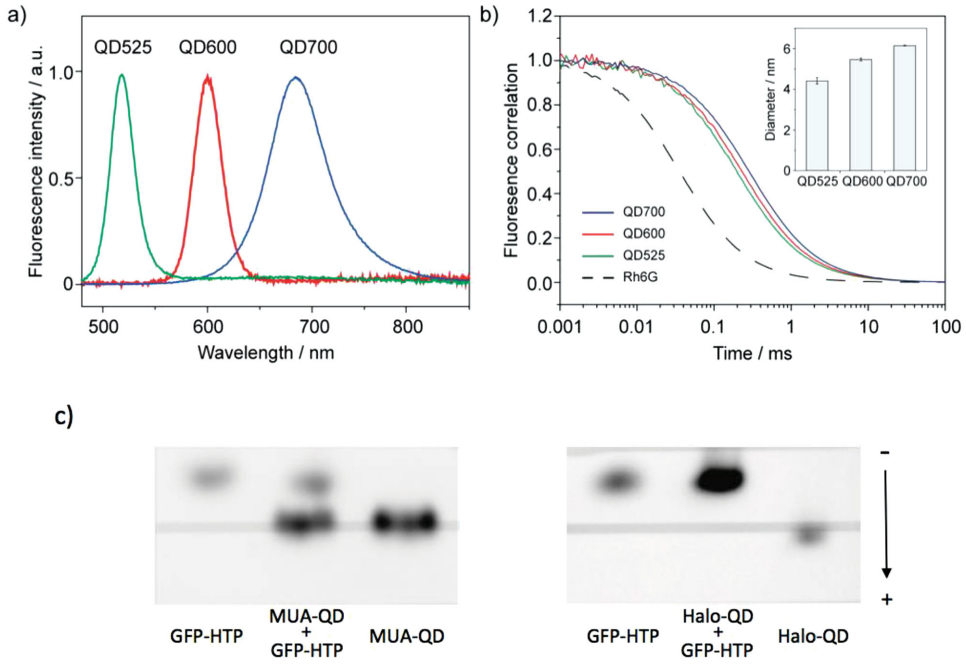

Figure 2. (a) Fluorescence spectra of Halo-QDs (QD525, QD600, and QD700) in water. (b) Fluorescence autocorrelation curves for the Halo-QDs and rhodamine 6G (Rh6G) in phosphate buffer (pH = 8). Inset shows the hydrodynamic diameter of the QDs, as determined by FCS measurements. (c) Agarose gel electrophoresis of MUA-QD and Halo-QD (QD600) in the absence and presence of GFP-HTP (QD: GFP-HTP = 1: 5 molar ratio). The fluorescence bands were detected using a longpass filter (>515 nm).

proteins. The addition of HTP fused green fluorescent proteins (GFP-HTP, 61 kDa) to the Halo-QDs resulted in 1.6-times increased in the QD size, indicating the formation of the complex between Halo-QDs and GFP-HTP molecules. In contrast, the hydrodynamic size of MUA-QDs did not change by addition of GFP-HTP (SI, Figure S3). Gel electrophoresis showed that the Halo-QDs formed complex with GFP-HTP with a single fluorescence spot, whereas MUA-QDs did not form the complex with GFP-HTP (Figure 2c). This result indicates that GFP-HTP molecules specifically bind to the HaloTag ligands presented on Halo-QDs. To evaluate the number of GFP-HTP molecules binding to one particle of Halo-QD, we measured the fluorescence emitted from a single Halo-QD·GFP-HTP complex using a total internal reflection fluorescence (TIRF) microscopy (**Figure 3**a). The fluorescence intensity of total GFP fluorescence signals in the Halo-QD·GFP-HTP complex was 1.9 times larger than that of a free GFP molecule (Figure 3b). Taking into account the effect of fluorescence energy transfer from GFP to Halo-QDs (SI, Figure S4) in the complex, the average number of GFP-HTP molecules conjugated to a single Halo-QD particle is estimated to be ca. 4.

We next conducted single-molecule fluorescence imaging using Halo-QDs (QD600) in HTP-cAR1 expressing living *Dictyostelium* cells (**Figure 4**a). When the cells were incubated with Halo-QDs, most QDs showed fluorescence blinking on the cell membrane, which is consistent with single-molecule

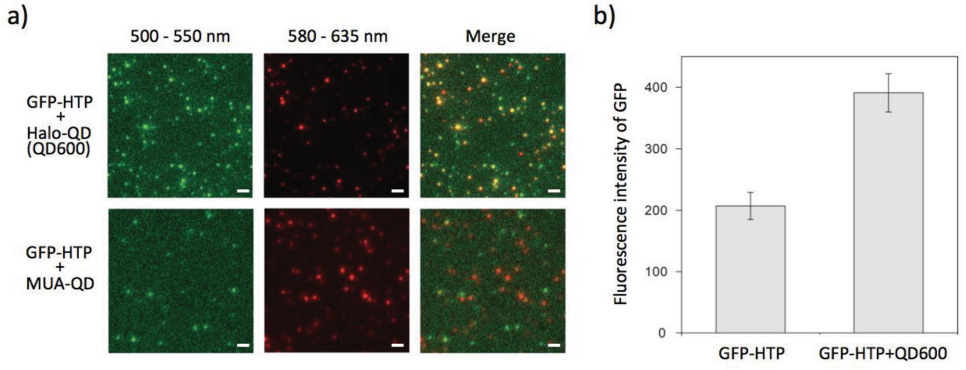

Figure 3. (a) Single-molecule fluorescence images of the colocalization of GFP-HaloTag fusion protein (GFP-HTP) and Halo-QD (QD600) particles on a glass surface. Fluorescence signals of GFP-HTP and Halo-QD (QD600) were observed at wavelengths of 500–550 nm and 580–635 nm, respectively. Five equivalent amounts of GFP-HTP were mixed with Halo-QD (QD600). TIRF microscopy images of GFP-HTP and MUA-QD (600 nm emission) mixtures are shown as a negative control. Scale bar: 1 μm. (b) Fluorescence intensities of GFP in single molecules of GFP-HTP and the complexes of GFP-HTP and Halo-QD (QD600), as measured by the single-molecule fluorescence images of (a).

DOI: 10.1002/smll.201402508

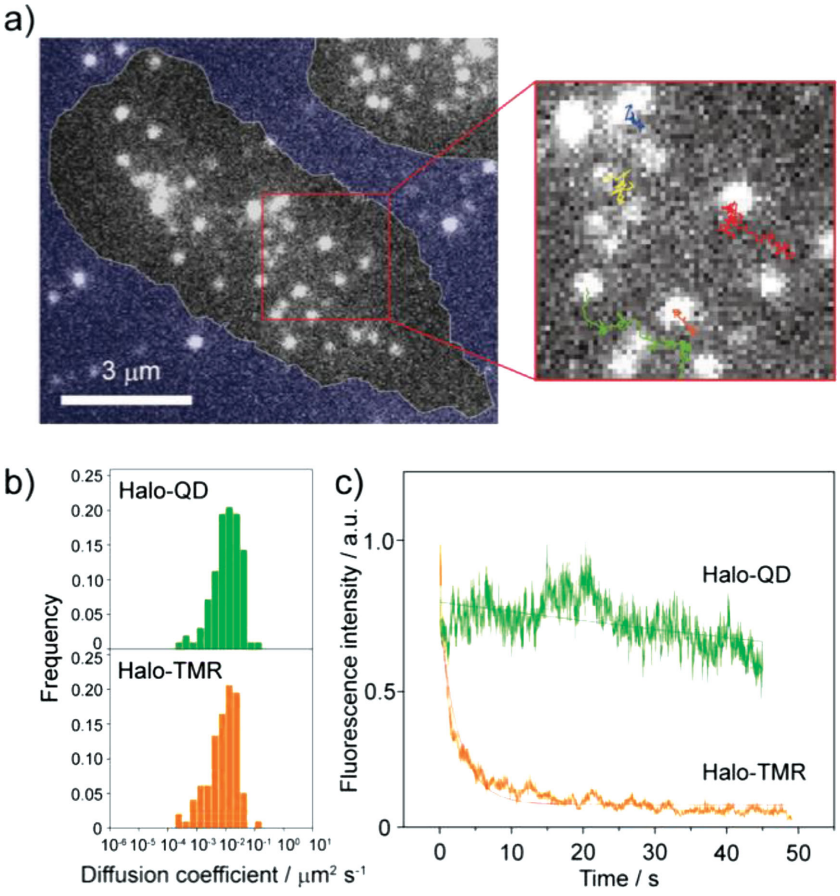

Figure 4. (a) Single-molecule fluorescence image of Halo-QD (QD600) labeled HTP-cAR1 receptors in living *Dictyostelium* cells. Single-molecule trajectories (magnified figure) of Halo-QDs for a ca. 5 s recording are shown. (b) Diffusion coefficients of the HTP-cAR1 receptors, as determined by single-molecule tracking using Halo-QD and Halo-TMR labels. (c) Fluorescence photobleaching of Halo-QDs and Halo-TMR molecules (ca. 50 particles) under the irradiation of a 561 nm laser.

observation of QDs (SI, Figure S5-S7 and Movie 1).[16] In contast, when the cells were incubated with MUA-QDs, significant fluorescence signals from the cells were not observed (SI, Figure S5). From the trajectories of the Halo-QD fluorescence signals, the diffusion coefficients of the QD labeled HTP-cAR1 molecules were calculated. Alternatively, we determined the diffusion coefficients of the HTP-cAR1 molecules using tertamethyl rhodamine labeled HaloTag-ligands (Halo-TMR, MW = 636).[17] The diffusion coefficient of HTP-cAR1 molecules, as determined by Halo-QDs, was 0.017 ± 0.002 $\mu m^2/s$, which is not significantly different from those determined by Halo-TMR (0.014 ± 0.002 $\mu m^2/s$) or a previously reported value[17] (Figure 4b). This finding indicates that the labeling with Halo-QD does not disrupt the diffusion of HTP-fused GPCR proteins on the cell surface. Additionally, it is noteworthy that the Halo-QD probes were highly resistant to photobleaching during single-molecule imaging. Figure 4c shows the time course of the fluorescence intensity of Halo-QDs and Halo-TMR molecules adsorbed on a cover glass under the irradiation of a 561 nm laser. Fluorescence of the Halo-TMR molecules was photobleached within 10 sec, while fluorescence of the Halo-QDs did not significantly decrease over a period of 1 min, showing that the Halo-QDs are photostable and suitable for long-term observation of single molecule trajectories.

In single molecule fluorescence imaging, the spatial resolution is restricted by the diffraction limit of the fluorescence emission wavelength, which is approximately 200 nm when using visible light.[18] Thus, by using one-colored single molecule fluorescence imaging, we cannot resolve the fluorescence spots emitted from probe-labeled proteins that are located at the area within ca. 200 nm. However, if we use multicolored single-molecule imaging, we can detect individual single molecules that exist in the area (<200 nm) by resolving the fluorescence emitting from different QDs. Using Halo-QDs with three different emissions, we succeeded in achieving multicolored single-molecule fluorescence imaging of HTP-fused cAR1 proteins in *Dictyostelium* cells (SI, Movie 2). To determine the position of GPCR proteins on the cell membrane, we fixed the cell with paraformaldehyde, and took single-molecule fluorescence images. **Figure 5**a shows the single-molecule image (>500 nm emission) of Halo-QDs (QD525, QD600 and QD700) labeled HTP-GPCR proteins. From this fluorescence image, we detected 85 fluorescence spots emitted from the QDs. Using three band-pass filters (SI, Figure S8), we could resolve the fluorescence signals from the three types of QDs. Figure 5b shows the fluorescence intensity line profiles of each QDs, which are obtained by using Gaussian functions. Multicolored single-molecule images revealed three times larger number (250) of GPCR molecules than one-colored single-molecule images did (Figure 5c). This result shows that multicolored single-molecule imaging can discriminate the GPCR membrane proteins existing in the optical diffraction limit.

In summary, we have demonstrated the capability of compact Halo-QDs for multicolored single-molecule imaging of GPCR proteins in living *Dictyostelium* cells. To prepare the Halo-QDs, we used thiol-terminated HaloTag ligands (Halo-SH) that directly bind to the surface of the QDs. An alternative method for preparing Halo-QDs is the conjugation of HaloTag ligands to QDs using carbodiimide cross coupling between MUA-QDs and amine-terminated HaloTag ligand (Halo-NH_2). Although this method is facile for preparing HaloTag ligand conjugated QDs, the control of amounts of HaloTag ligand on the QDs surface is very difficult. This is because that the conjugation efficiency strongly dependent on the reaction condition such as the concentrations of reactants (QDs, Halo-NH_2, and coupling reagents), pH, and reaction time. In contrast, direct conjugation of HaloTag ligand (Halo-SH) to QD surface is highly reproducible for preparing HaloTag conjugated QDs that can be used for a single molecule imaging

small 2014,
DOI: 10.1002/smll.201402508

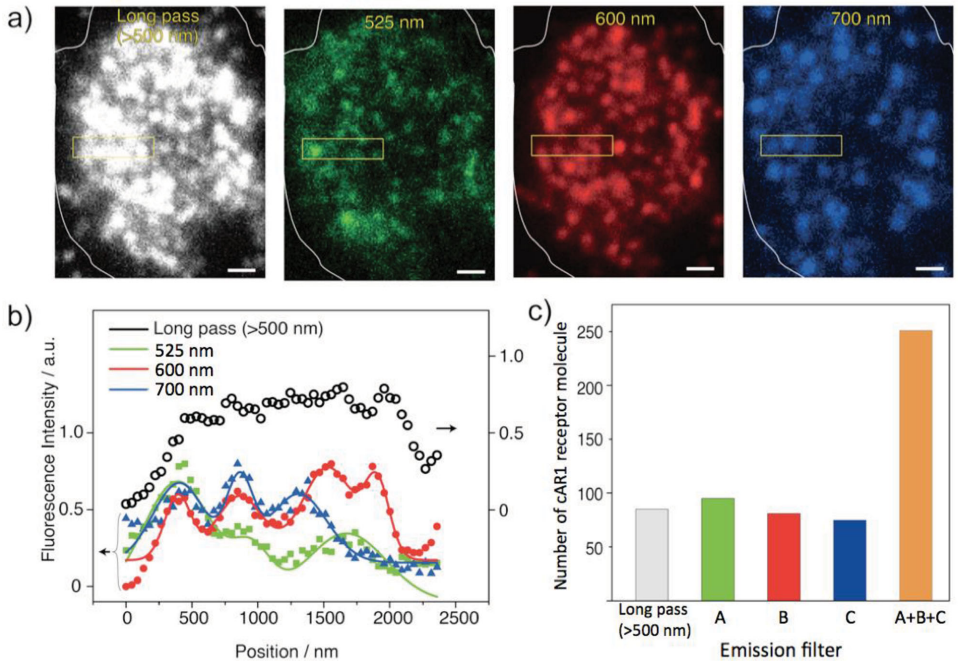

Figure 5. (a) One-colored (>500 nm) and multicolored (with emission filters) single-molecule fluorescence images of Halo-QDs (QD525, QD600, and QD700) labeled HTP-cAR1 receptors in a *Dictyostelium* cell. Scale bar: 1μm. (b) Fluorescence intensity line profiles of the Halo-QDs shown in the yellow rectangles of the images in a). (c) The number of HTP-cAR1 receptor on the cell surface, as determined by the analysis of one-colored (long pass >500 nm) and multi-colored single-molecule fluorescence images using emission filters A (525 nm), B (600 nm), and C (700 nm).

of GPCR proteins in *Dictyostelium* cells. Our Halo-QDs as a single-molecule imaging probe have several advantages such as compact-size (<6 nm), high colloidal disepersibilty, and specific binding ability to HTP molecules. Using the Halo-QDs, multicolored single-molecule imaging of HTP fused GPCR molecules can be achieved for the detection of individual GPCR molecules existing in the optical resolution limit. By three-colored single-molecule imaging, we could detect the number of GPCR proteins by a factor of 3 than one-colored single-molecule imaging did. The compact Halo-QDs will be useful for the study of membrane protein dynamics using multicolored single-molecule fluorescence imaging.

Supporting Information

Supporting Information is available from the Wiley Online Library or from the author.

Acknowledgements

We are grateful to Peter Karagiannis (QBiC, RIKEN) for critical reading of this manuscript and Seiya Fukushima (Osaka Univ.) for constructing a TIRF microscopy. We are also grateful to Miyuki Hasegawa for preparing GFP-HaloTag fusion proteins.

[1] M. J. Saxton, K. Jacobson, *Annu. Rev. Biophys. Biomol. Struct.* **1997**, *26*, 373–399.
[2] C. Joo, H. Balci, Y. Ishitsuka, C. Buranachai, T. Ha, *Ann. Rev. Biochem.* **2008**, *77*, 51–76.
[3] a) M. Bruchez Jr., M. Moronne, P. Gin, S. Weiss, A. P. Alivisatos, *Science* **1998**, *281*, 2013–2016; b) W. C. W. Chan, S. Nie, *Science* **1998**, *281*, 2016–2018; c) X. Michalet, F. F. Pinaud, L. A. Bentolila, J. M. Tsay, S. Doose, J. J. Li, G. Sundaresan, A. M. Wu, S. S. Gambhir, S. Weiss, *Science* **2005**, *307*, 538–544.
[4] a) X. Wu, H. Liu, J. Liu, K. N. Haley, J. A. Treadway, J. P. Larson, N. Ge, F. Peale, M. P. Bruchez, *Nat. Biotechnol.* **2003**, *21*, 41–46; b) J. K. Jaiswal, H. Mattoussi, J. M. Mauro, S. M. Simon, *Nat. Biotechnol.* **2003**, *21*, 47–51; c) D. K. Tiwari, S. Tanaka, Y. Inouye, K. Yoshizawa, TM. Watanabe, T. Jin, *Sensors* **2009**, *9*, 9332–9354.
a) M. Dahan, S. Lévi, C. Luccardini, P. Rostaing, B. Riveau, A. Triller, *Science* **2003**, *302*, 442–445; b) D. S. Lidke, P. Nagy, R. Heintzmann, D. J. Arndt-Jovin, J. N. Post, H. E. Grecco, E. A. Jares-Erijman, T. M. Jovin, *Nat. Biotechnol.* **2004**, *22*, 198–203; c) C. Bouzigues, M. Morel, A. Triller, M. Dahan, *Proc. Natl. Acad. Sci. U.S.A.* **2007**, *104*, 11251–11256; d) K. M. S. O'Connell, A. S. Rolig, J. D. Whitesell, M. M. Tamkun, *J. Neurosci.* **2006**, *26*, 9609–9618; e) M. M. Tamkun, K. M. S. O'Connell, A. S. Rolig, *J. Cell. Sci.* **2007**, *120*, 2413–2423; f) I. R. Bates, B. Hébert, Y. Luo, J. Liao, A. I. Bachir, D. L. Kolin, P. W. Wiseman, J. W. Hanrahan, *Biophys. J.* **2006**, *91*, 1046–1058; g) H. Chen, I. Titushkin, M. Stroscio, M. Cho, *Biophys. J.* **2007**, *92*, 1399–1408; h) G. C. Kodippili, J. Spector, C. Sullivan, F. A. Kuypers, R. Labotka, P. G. Gallagher, K. Ritchie, P. S. Low, *Blood* **2009**, *113*, 6237–6245; i) F. Pinaud, S. Clarke, A. Sittner, M. Dahan, *Nat. Methods* **2010**, *7*, 275–285.
[5] Technical Manual Promega, "HaloTag Technology: Focus on Imaging", http://www.promega.com, **2013**, accessed: August 2014.
[6] G. V. Los, L. P. Encell, M. G. McDougall, D. D. Hartzell, N. Karassina, C. Zimprich, M. G. Wood, R. Learish, R. F. Ohana, M. Urh, D. Simpson, J. Mendez, K. Zimmerman, P. Otto, G. Vidugiris, J. Zhu, A. Darzins, D. H. Klaubert, R. F. Bulleit, K. V. Wood, *ACS Chem. Biol.* **2008**, *3*, 373–382.

[7] D. S. Liu, W. S. Phipps, K. H. Loh, M. Howarth, A. Y. Ting, *ACS Nano* **2012**, *6*, 11080–11087.
[8] Y. Zhang, M. So, A. M. Loening, H. Yao, S. S. Gambhir, J. Rao, *Angew. Chem. Int. Ed.* **2006**, *45*, 4936–4940.
[9] M. So, H. Yao, J. Rao, *Biochem. Biophys. Res. Commun.* **2008**, *374*, 419–423.
[10] M. Ueda, Y. Sako, T. Tanaka, P. Devreotes, T. Yanagida, *Science* **2001**, *294*, 864–867.
[11] Y. Miyanaga, S. Matsuoka, M. Ueda, *Methods Mol. Biol.* **2009**, *571*, 417–435.
[12] P. S. Klein, P. J. Sun, C. L. Saxe III, A. R. Kimmel, R. L. Johnson, P. N. Devreotes, *Science* **1988**, *241*, 1467–1472.
[13] a) B. O. Dabbousi, J. Rodriguez-Viejo, F. V. Mikulec, J. R. Heine, H. Mattoussi, R. Ober, K. F. Jensen, M. G. Bawendi, *J. Phys. Chem. B.* **1997**, *101*, 9463–9475; b) T. Jin, F. Fuji, Y. Komai, J. Seki, A. Seiyama, Y. Yoshioka, *Int. J. Mol. Sci.* **2008**, *9*, 2044–2061; c) T. Jin, Y. Yoshioka, F. Fujii, Y. Komai, J. Seki, A. Seiyama, *Chem. Commun.* **2008**, 5764–5666; d) T. Jin, A. Sasaki, M. Kinjo, J. Miyazaki, *Chem. Commun.* **2010**, *46*, 2408–2410.
[14] a) Y. Nakane, Y. Tsukasaki, T. Sakata, H. Yasuda, T. Jin, *Chem. Commun.* **2013**, *49*, 7584–7586; b) M. Hasegawa, Y. Tsukasaki, T. Ohyanagi, T. Jin, *Chem. Commun.* **2013**, *49*, 228–230; c) Y. Nakane, A. Sasaki, M. Kinjo, T. Jin. *Anal. Methods* **2012**, *4*, 1903–1905.
[15] M. Nirmal, B. O. Dabbousi, M. G. Bawendi, J. J. Macklin, J. K. Trautman, T. D. Harris, L. E. Brus, *Nature* **1996**, *383*, 802–804.
[16] a) X. Xu, T. Meckel, J. A. Brzostowski, J. Yan, M. Meier-Schellersheim, T. Jin, *Sci. Signal.* **2010**, *3*, ra71; b) J. Lee, Y. Miyanaga, M. Ueda, S. Hohng, *Biophys. J.* **2012**, *103*, 1691–1697.
[17] a) TM. Watanabe, S. Fukui, T. Jin, F. Fujii, T. Yanagida, *Biophys. J.* **2010**, *99*, L50–L52; b) D. K. Tiwari, T. Nagai, *Develop. Growth Differ.* **2013**, *55*, 491–507.

Received: August 21, 2014
Revised: September 19, 2014
Published online:

DOI: 10.1002/smll.201402508